SAR Patterns of Invasive and Non-invasive Antenna Array in Combination of Hyperthermia and Radiation Brachytherapy

University of Tokyo	Oiendrila B DEBNATH	Non-Member
Chiba University	Kazuyuki SAITO	Non-Member
Chiba University	Koichi ITO	Non-Member
University of Tokyo	Mitsuru UESAKA	Member

Abstract

Combination of Microwave Hyperthermia and Radiation Therapy is effective for treatment of tumor. After increasing the temperature the tumor becomes more sensitive to radiation dose. In this paper, the Invasive and Non-invasive microwave antennas were designed and applied on different tissues including malignant tumor, and respective Specific Absorption rate (SAR) patterns and temperature rises were investigated. For invasive antenna, coaxial-slot antennas was investigated and for non-invasive antenna, micro strip patch antenna and spiral antenna were investigated. The objective in the current phase of research work is to find the most optimum antenna array which can be effectively used for breast tumor with minimal impact on the adjacent tissues.

Both theory and experiment demonstrated that the maximum SAR occurred in the junction plane of antenna arrays. These experiments have been conducted using a frequency of 2.45GHz.

Keywords: Antenna array, Microwave hyperthermia, Radiation dose, Specific absorption rate

1. Introduction

Microwave-hyperthermia is a method of treating cancer by heating the tumor. Once a tumor is heated, either it dies or becomes more sensitive to radiation brachytherapy using radioisotopes. Thus, with an appropriate rise in temperature by hyperthermia, the conventional radiation dose can be minimized [1], and a combination of these two methods can be more effective in reduction of tumor [2]. By use of an appropriate antenna array, temperature rise to about 42°C-45°C is achieved. The primary motivation of this paper is to evaluate the characteristics of invasive and non-invasive antenna array on several kinds of tissue.

連絡先:Oiendrila B Debnath,
〒113-8654, Bunkyo-ku, 7-3-1 Hongo
University of Tokyo
E-mail: oiendrila.bhowmik@nuclear.jp

For invasive antenna, geometry parameters and the slots were chosen for the frequency 2.45GHz [3] and for non-invasive antenna the antenna parameters were calculated for same frequency. The structure of a two slot coaxial-slot antenna is shown in Figure 1.

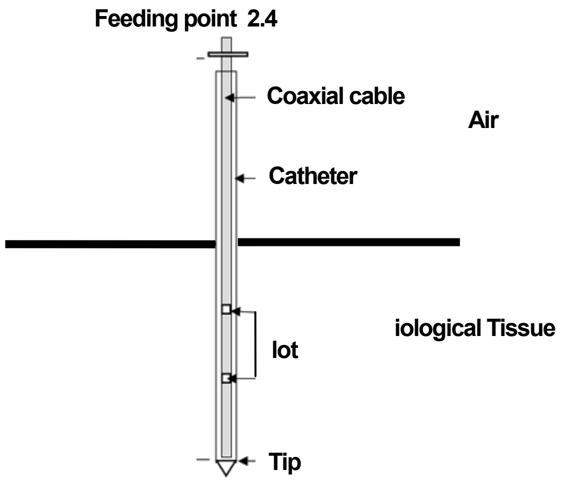

Figure. 1 Coaxial slot antenna ith t o slots

2. Description of the Antenna array

The structure of micro strip patch antenna is shown in Figure 2.

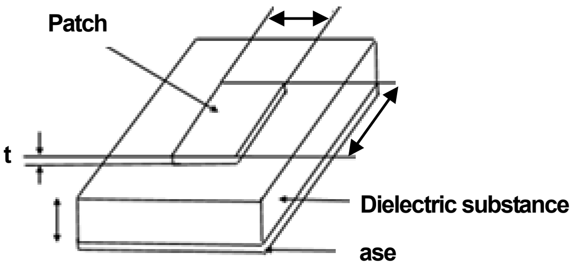

Figure. 2 icro strip patch antenna structure

The material for spiral antenna was the same as that of micro strip patch antenna. The structure of spiral antenna is shown in Figure 3.

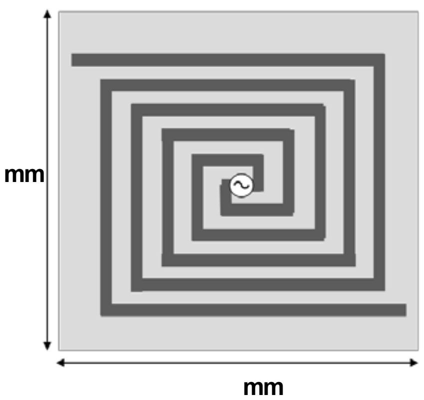

Figure. 3 piral antenna structure

3. Calculation for SAR and temperature

The basic concept for determining SAR relies on the fact that the tissue or phantom material when exposed to electromagnetic radio waves, absorbs power and this power gets distributed throughout the tissue or phantom material. This SAR is defined by Equation 1.

$$|SAR| = \sigma.\frac{|E|^2}{\rho} \qquad \text{Equation (1)}$$

Where σ is the conductivity of the tissue (S/m), ρ is the density of the tissue (kg/m^3), and |E| is the electric field (V/m). Value of SAR is different for different tissue phantoms and for different antenna array structure. The SAR was calculated for muscle, fibro glandular tissue and tumor tissue. The electromagnetic field was calculated around the antenna by use of FDTD calculations [4]. Table 3 gives the values used in FDTD calculations.

Table 3 Description of FDTD calculation

Description in mm	alue	
Cell si e inimum $\Delta x, \Delta y, \Delta z$	.	1. as constant
Cell si e aximum $\Delta x, \Delta y, \Delta z$	1.	

The relative permittivity and conductivity of these tissue phantoms are given in Table 4.

Table 4 alues for each of the biological tissues examined

Tissue phantom	elative permittivity	Conductivity
in	1.	4 .24
Fat	.21	. 4
Fibro glandular tissue	1. 3	44.
alignant tumor	2. 1	2.

Temperature rise inside the tumor due to application of coaxial-slot antenna array was also calculated. Thermal models, such as the Penne' s Bio heat model [5] and Chen Holmes Model [6] were established. The Penne' s model for describing heat transfer in a tissue, known as the "bio-heat transfer" equation [5], is shown in Equation 2. This equation was used to calculate temperature. Body temperature was considered to be 37°C.

$$(\rho.c_p)_t \frac{\partial T_t}{\partial t} = \nabla.(k_t.\nabla T_t) + q_p + q_m \qquad \text{Equation (2)}$$

Where ρ, c_p, T_t, k_t, q_p, q_m are tissue density, tissue-specific heat, tissue temperature, tissue thermal conductivity, heat transfer from blood to tissue, and uniform rate of metabolic heat generation in the tissue layer per unit volume, respectively. Equation 3 describes the boundary condition.

$$-k_t.\nabla T_t = H(r).\nabla T_t + 40.6(S.W + P.I)/S \qquad \text{Equation (3)}$$

Where H, T_t denote, respectively, the heat transfer coefficient, difference between the body surface temperature and air temperature. The heat transfer coefficient includes the convective and radiative heat losses. S is the total surface area of the human body, S.W [g min^{-1}] is the sweating rate, and P.I is the water loss. The temperature of blood varies according to the first law of thermodynamics [6, 7]. Equation 4 describes the change in temperature of blood.

$$T_B(t) = T_{B0} + \int_t \frac{Q_{BTN}(t)}{C_p \rho V} dt$$ Equation (4)

Where Q_{BTN} is the net rate of heat acquisition in the body tissues from blood, C_p is the specific heat of blood, ρ is the mass density and V is the total volume of blood. Thermal conductivity of material used in antenna was calculated using Equation (5) which was derived from Maxwell's equations.

$$\frac{J_c}{\sigma_s} = \frac{D}{\epsilon}$$ Equation (5)

Where Jc, σ_s, D, ϵ are electric current density, thermal conductivity, electric flux density and relative permittivity of the material respectively.

4. Use of bolus material

Bolus material is an important factor while using non-invasive antennas on the body to generate resonance at a particular frequency. For non-invasive antennas, far field is generated inside the tissue and as a result the temperature is elevated. Bolus material is necessary to avoid skin ablation. In this research, three types of bolus materials were used, namely normal water, saline water and distilled water. Among these, distilled water gave the best result. The temperature elevation in the surface of the skin with and without bolus material is shown in Figure 4.

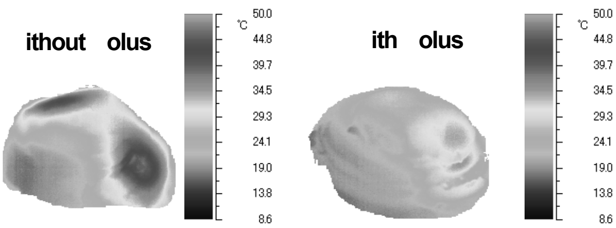

Figure 4. nfra red images of breast tumor ith and ithout bolus material

5. Results

The power distribution from two coaxial-slot (invasive) antennas on the tumor phantoms was observed in CST simulation and in experiments conducted. The pattern is developed around the slots. In this particular coaxial-slot antenna, two slots were made to achieve efficient heating. Figure 5 shows the SAR distribution of coaxial-slot antenna array inside the breast tumor phantom. SAR of other tissues such as fibro glandular tissue, muscle were also calculated.

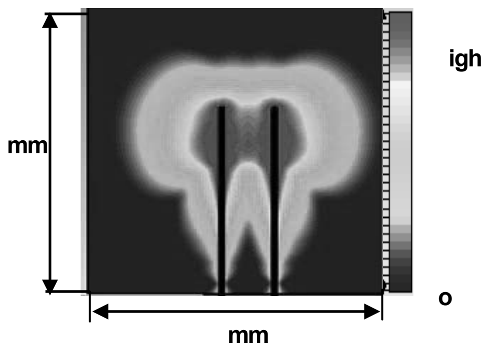

Figure. A distribution of the coaxial slot antenna array in tumor phantom

Figure 6 shows the SAR distribution from micro strip patch antenna applied on breast tumor phantom. Further, the SAR was found to be maximum at the junction of the antenna array.

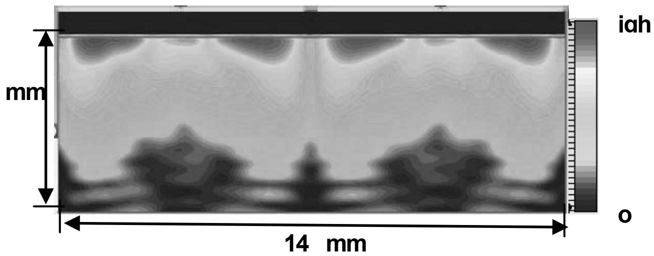

Figure. A distribution from t o micro strip patch antennas applied on tumor phantom

Spiral antenna radiates in a perpendicular direction. On the application of spiral antenna array, the SAR as well as the rise in temperature is more as compared to those of micro-strip patch antenna. Figure 7 shows the SAR distribution from spiral antenna applied on breast tumor phantom.

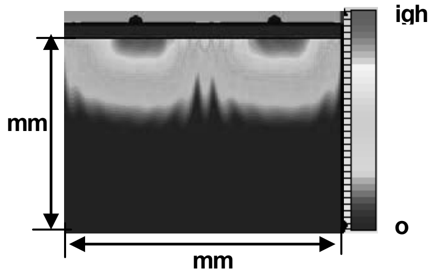

Figure. A distribution from t o spiral antennas applied on tumor phantom

The antennas in all the cases were separated by 0.5cm, and a power of 25watt was used.

6. Conclusion

Hyperthermia helps to increase the temperature of the tissues to around 42°C -45°C and in combination with radiation brachytherapy can effectively reduce the conventional dose. For both types of non-invasive antennas a bolus material was used for avoiding skin ablation. For micro strip patch antenna, the temperature rise was about 4°C after 18 minutes of heating; for spiral antenna, about 7°C after 15 minutes of heating; for invasive antenna, about 8°C after 10 minutes of heating. Also for the non-invasive antennas the maximum power generation was observed within 3 cm below the surface where the antenna array was applied. Thus, for a case of deep seated tumor, these non-invasive antennas cannot ensure a temperature rise of the tumor in tumor. The diffraction is much lesser for coaxial-slot antenna. Though the time is taken more, no adjacent tissues are heated and after the coaxial-slot antenna's application, a lower dose of radiation is expected to be effective for breast tumor. In conclusion, the efficiency of the coaxial-slot antenna is more because of the power generated in a localized region and ability to control the position of the antenna array inside the tissue.

Future work will focus on calculating the radiation dose distribution by radiation brachytherapy and optimizing the combination of hyperthermia and radiation dose distribution for breast tumor.

References

[1] P Kaur : 'Combined hyperthermia and radiation therapy for cancer'. Cancers; doi:10.3390/cancers3043799, 2011

[2] Jacob D Shea.: 'Microwave imaging of realistic numerical breast phantoms" Medical Physics, Vol. 37, No. 8, August 2010

[3] Saito. K, 'Clinical trials of interstitial microwave hyperthermia by use of coaxial antenna with two slots'; IEEE Transactions on Microwave Theory and technoques, vol.52, No.8, August 2004.

[4] H. H. Pennes, "Analysis of tissue and arterial temperature in the resting human forearm," J. Appl. Physiol., vol. 1, pp. 93-122, 1948

[5] M. M. Chen, K. R. Holmes, and V. Rupinskas, "Pulse-decay method for measuring the thermal conductivity of living tissues," ASME J. Biomech. Eng., vol. 103, pp. 253-260, 1981.

[6] P. Bernardi, M. Cavagnaro, S. Pisa and E. Piuzzi, "Specific absorption rate and temperature elevation in a subject exposed in the far-field of radio-frequency sources operating in the 10-900-MHz range," IEEE Trans. Biomed. Eng., vol.50, pp.295-304, 2003.

[7] A. Hirata and O. Fujiwara, "Modeling time variation of blood temperature in a bioheat equation and its application to temperature analysis due to RF exposure," Phys. Med. Biol. Vol.54, pp.N189-196, 2009.